Sediment accumulation in a manipulated bay of Puget Sound, Bellingham, WA.

Mary Alice Benson

A report prepared in partial fulfillment of
the requirements for the degree of

Master of Science
Earth and Space Sciences: Applied Geosciences

University of Washington
June 2019

Project mentors:
Charles Nittrouer, University of Washington School of Oceanography
Aaron Fricke, University of Washington School of Oceanography

Reading committee:
Juliet Crider
Charles Nittrouer

MESSAGe Technical Report Number: 074

Abstract

Mud Bay, located in Bellingham, Washington at the north end of Chuckanut Bay, is filling with sediment at a rate greater than projected sea-level rise. This is worrisome as the bay is an important habitat for eelgrass meadows, shellfish beds, and birds. Also, Chuckanut Creek, the primary fluvial input into the bay, has historically been a salmon-spawning ground. In 2013 the City of Bellingham identified this bay and pocket estuary as a top-ranked 10-year restoration priority due to degradation of wildlife habitat from sediment accumulation. Anthropogenic stressors that could increase sediment accumulation include logging, mining and quarrying in proximal areas during the late 1800s to early 1900s. In the 1920s a rip-rap railroad causeway was constructed across the mouth of the bay, limiting tidal and storm wave energy. During the construction of Interstate 5 in the early 1960s, additional sediment could have been transported to the bay by Chuckanut Creek. To determine if the bay is filling, I collected cores from 4 sites in the intertidal zone of the study area, near where Chuckanut Creek enters the bay. Using ^{210}Pb, I calculated the accumulation rates to range from 0.20 to 1.07 cm yr^{-1}, with spatial variations attributed to differences in tidal and fluvial energy at each coring location. This accumulation rate was corroborated using ^{137}Cs at one coring site, and depth-of-penetration values for both radiochemical analyses agree. All ^{210}Pb profiles indicated constant accumulation rates, and a link between increased accumulation and construction of the causeway was not found. Grain-size analyses and X-radiography images were used to interpret sedimentation patterns in the bay. Grain-size distributions indicate that the east side of the bay is finer grained. There is potentially a sediment signature that can be linked to the construction of Interstate 5. Sea level has risen by 0.12 cm yr^{-1} since 1934 and relative sea-level projections range from ~0.38 to 0.71 cm yr^{-1} by 2100 so accommodation space has, and continues to, fill faster than sea-level rise in the bay.

Table of Contents

List of figures

Acknowledgements:

I would like to thank:

Elizabeth Wratten for her willingness to join me in researching Mud Bay, allowing me to bouncing ideas off her, and for just being amazing.

Charles Nittrouer and Aaron Fricke for sharing their knowledge, field and laboratory equipment, and enthusiasm with me.

Juliet Crider and Charles Nittrouer for their ideas and editing feedback that helped transform this paper into a readable version.

Elizabeth Davis, Carrie Garrison-Laney, Chelsea Bush, Morgan Simon and Duane Beaman for joining me in the field.

Jo and Denny Miller for providing a home base in Chuckanut Village, and for allowing me to borrow their dog Scout for scale.

Wayne and Laura Gerner for sharing verbal history of the bay, and for allowing me to use their driveway during field days.

Robin McLachlan, Hannah Glover and everyone else in the Sediment Dynamics Group at the University of Washington School of Oceanography for helping troubleshoot technology issues, and for their flexibility in sharing laboratory space and resources.

The Whatcom County Museum for providing me access to, and the use of, the historical photographs used in this paper.

Introduction

Mud Bay is a small bay in Bellingham Washington that has undergone anthropogenic modifications over the last century. It is an important natural wildlife habitat, and the City of Bellingham (COB) is concerned that human alterations to the bay are negatively affecting this area, resulting in increasing sediment accumulation. To my knowledge, no prior quantitative assessments of sediment accumulation have been published for Mud Bay. The purpose of this study is to quantify accumulation rates and grain-size distribution in the bay to determine if it is filling, if sedimentation patterns have changed over the last century, and if I can directly link a change in sedimentation to anthropogenic modifications.

1.0 Background:

1.1 Geographic Setting

Mud Bay is located on the northeast coast of Puget Sound, in Bellingham, Washington (fig. 1). It is a small recessed embayment in the northernmost section of Chuckanut Bay (fig. 2), with an ~10-m natural bathymetric break at the mouth of Mud Bay (Pritchett, 1898). Gilbert described the bay as shallow in the 1887 U.S. Coast and Geodetic Survey. The earliest nautical map available does not give a depth for the bay, indicating that it was not navigable by ships. (Pritchett, 1898). The bay is enclosed by cliffs to the west and east, with a Broad fluvial valley entering from the north. Chuckanut Creek drains through this valley into Mud Bay (Fig. 3).

The primary fluvial input into Mud Bay is Chuckanut Creek. The headwaters of Chuckanut Creek originate in the foothills of Lookout Mountain, to the north of the bay, at an elevation of ~366 m (fig. 3). It traverses ~10 km to its mouth, near sea level in Mud Bay. The mouth of Chuckanut Creek is located on a 100-year floodplain, with a 26% chance of a flood event over 30 years, but the area is not identified as a frequently flooded area (COB, 2019). There is no defined base flood elevation, and stream-gauge data for this creek initiate during water year 2005. There are

no historic flood records for the creek (Michelle Evans, COB Public Works Department, personal communication, 2019). For most of its course Chuckanut Creek flows through a narrow ravine, with 20% gradients to near-vertical walls on the side slopes. These gradients shallow in Chuckanut Village, allowing for some meander (COB, 2011). The lower reach of Chuckanut Creek is categorized as a pocket estuary (Eissinger, 1995; Northwest Ecological Service, 2006).

1.2 Geology

The Mud Bay area is dominated by two geologic units, the Chuckanut Formation and Pleistocene glacial drift (Easterbrook, 1976). The cliffs adjacent to the bay are part of the Padden Member of the Chuckanut Formation (Johnson, 1982). The Padden Member is an alluvial deposit, up to 3000 meters thick, that dates from middle to late Eocene (Johnson, 1982). It contains sandstones, mudstones and conglomerates. The area was last glaciated during the Vashon Stade, with glaciation reaching a maximum extent ~15,000 years ago, and then retreating rapidly (Mullineaux, 1965). The glacial deposit seen in the valley along the banks of Chuckanut Creek is a clay-rich gravelly till, identified as undifferentiated glacial drift on geologic maps (Easterbrook, 1976).

The Bellingham area is still undergoing isostatic rebound at an average of 0.03 ±0.12 cm yr^{-1} (Washington Coastal Hazards Resilience Project, 2018). Sea-level rise since 1934 has been 0.12 ±0.027 cm yr^{-1} (NOAA, 2018). Future relative sea-level rise is estimated to range from ~0.38 cm yr^{-1} to 0.71 cm yr^{-1} by 2100 (Mazzotti et al., 2008; Washington Coastal Hazards Resilience Project, 2018).

1.3 Anthropogenic influences

The area surrounding Mud Bay has been dominated by industrial and residential use for over a century, some of which might have generated additional sediment that could have been transported into the bay. Logging on Chuckanut Ridge was done from the 1890s to around 1915

(Davis, 1993). The bay was used for log boom storage from the early 1900s into the 1920s (figs. 4 and 5). Above Teddy Bear Cove, ~0.5 km south of Mud Bay, a brick and tile factory operated intermittently during 1915-1925. The section of Chuckanut Drive above Mud Bay was constructed from 1920-1921 (Thomas, 1971).

Additional nearby extractive industries included the Chuckanut Stone Quarry which was operational from 1880-1908 and was located ~13 km south of Mud Bay. Two one-man coal mining operations were in existence during the early 1900s. One was located ~3 km south of Mud Bay on Governors Point and was operational during 1921-1922. The other was of unknown location or operational date. Both mines contained low-grade coal and were not considered highly productive (Thomas, 1971). There was also a salmon cannery south of the quarry during 1900-1934 (Thomas, 1971). While these exemplify industrial activities in the near vicinity, none of these specific examples is likely to have influenced the sediments in Mud Bay.

Local uses also required workers, who needed housing. Chuckanut Village, located at the north end of the bay, was already platted by 1891 (Lewis and Alberton, 1891). The intertidal zone was also platted but was never developed. Chuckanut Village was originally built as housing for the workers of the above industries, but people continued to live there after the industries disappeared (Farrow et al., 1989). Additional housing developments have been built on the west side of the bay, beginning with the Chuckanut Bay Subdivision, approved for construction in 1984 (Ted S. Gacek & Associates, 1984). Land-clearing and paving associated with urbanization could increase the sediment transported into the bay.

The engineered structure that has been most cited as the cause of increased sediment accumulation is the railroad causeway across the mouth of the bay (Farrow et al., 1989; COB, 1995; Eissinger, 1995; Wahl, T. 2008; MacLennan et al., 2013 a and b; Josephine Miller and Wayne Gerner, Chuckanut Village residents, personal communications, 2017). The Great

Northern Railway conducted a preliminary survey of their route in 1896 and opened a wooden railroad trestle across the mouth of the bay in 1904 (fig. 4) (Thomas, 1971, Farrow et al., 1989, Wahl, 2008). In the 1920s, this open-framework trestle was replaced by a rip-rap causeway with a 69-m-wide tidal inlet opening (fig. 6). The hypothesis is that reducing the bay mouth to this opening limited tidal and wave energy in the bay, and sediment began to accumulate in the intertidal zone. On the west side of Mud Bay there are wave-erosion features recorded in boulders of Chuckanut Formation sandstone (fig. 7). These features were first described by Gilbert as having an "infinite variety of fantastic shapes" caused by wind and wave action (1878). The bay has an ~14-km fetch, but large storm waves now break on the causeway, and do not enter the bay at full force (Wahl, 2008; Josephine and Dennis Miller, Chuckanut Village residents, personal communications, 2019).

The construction of Interstate 5 has also potentially affected sedimentation in Mud Bay, if only for a limited time (Northwest Ecological Services, 2006; Wahl, 2008). Construction took place from 1955 to 1966, with the last completed portion located directly upslope of Chuckanut Creek, ~1.6 km north of Mud Bay (Hillegas, 2004). Anecdotal evidence from people who lived in Chuckanut Village during construction states that the creek was the color of 'chocolate milk' due to the suspended sediment being transported (Josephine Miller and Wayne Gerner., Chuckanut Village residents, personal communications, 2017). This claim is plausible based on photographs of the grading during Interstate 5 construction, where large amounts of loose sediment were generated (fig. 8).

1.4 Environmental importance

Mud Bay is an important natural habitat. Eel grass meadows that serve as nursery environments for salmonids and other fish, as well as shellfish beds, are in the bay (Eissinger, 1995; Eissinger, 2003; Northwest Ecological Services, 2006; MacLennan et al., 2013 a and b). The estuary also

contains a salt marsh (Eissinger, 1995; Eissinger, 2003; Northwest Ecological Services, 2006; MacLennan et al., 2013 a and b). Chuckanut Creek and Mud Bay are spawning and rearing grounds for chum and coho salmon, steelhead trout, and sea-run cutthroat trout (Eissinger, 2003; Northwest Ecological Services, 2006; MacLennan et al., 2013 a and b). Migratory, wintering and resident species of birds use the bay, including bald eagles, osprey, and herons (Eissinger, 2003; Northwest Ecological Services, 2006). In 2009, the North Cascades Audubon Society published a list of 124 species of birds found in or around the bay over the previous year. Eissinger described the bay as "One of the most biologically significant marine habitat areas in Whatcom County (1995)." The bay and estuary have been identified in the COB Water Resource Inventory Area 1 Nearshore and Estuarine Assessment report as a top-ranked ten-year restoration priority due to degradation of habitat caused by sediment accumulation (MacLennan et al., 2013 a and b). Their recommendation is to either open or modify the causeway in order to increase tidal flushing and remove sediment from the bay.

2.0 Methods:

2.1 Field

Sediment cores were collected from four different locations in the bay (fig. 9) (Appendix A). These locations were chosen based on accessibility during low tide, areas inferred to have limited human activity, and proximity to Chuckanut Creek, tidal channels, and the causeway opening. All cores were collected from the intertidal zone from the central and east areas of the bay, distal to the shellfish harvesting activity which typically occurs to the west. Coring site 1 was located near the mouth of Chuckanut Creek at the top of an ~1-m-high cut bank. Coring site 4 was also ~1 m above, but more laterally distant from the creek. Coring sites 2 and 3 were located adjacent to, and at about the same elevation as, Chuckanut Creek tide-flat channels. Sites 1 and 4 are more distal from the causeway opening than sites 2 and 3 (fig. 10). There were three collection days between May and September 2018, with low tides ranging from +21.0 cm to

-47.5 cm.

To collect sediment cores, I used the following equipment: a ½-diameter gouge corer, a Russian peat corer, X-radiography trays, and a 15-cm-diameter push corer. Based on the assumption that Mud Bay accumulation rates would be similar to sediment accumulation rates of 0.2 cm yr^{-1} from the intertidal zone at Willapa Bay near Long Beach, Washington (Boldt et al., 2013), I collected initial cores to 50 cm depth below the bed surface with the expectation of capturing the historical changes in the bay. The Willapa Bay accumulation-rate estimate was a useful starting point, but fluvial and tidal conditions differ in the two bays, so the comparison was not robust. Even allowing for accumulation rates 1.5 times greater than the initial estimates, 50 cm was not sufficient to capture a full century. Collection depths were increased to 1 m when I determined that the accumulation rates were greater than 0.50 cm yr^{-1} in some areas of the bay.

Sediment from the ½-diameter corer was sectioned in the field, and put into sample bags as 2-cm increments to 20 cm depth, 5-cm intervals from 20 to 70 cm depth, and 10-cm increments to 100 cm depth. This allows for higher resolution at shallow depths, where identification of the surface mixed layer is important for analysis. Samples from this coring device were intended for ^{210}Pb analyses. Relatively complete ~100-cm cores were collected at sites 1 and 4. At site 2, a 50-cm core was collected during the first field visit. At site 3, an 80-cm core was collected. Sites 2 and 3 were sandier, which made coring more difficult and could account for the incomplete collection at site 3.

Russian peat cores were collected at sites 1, 2, and 4 down to 50-cm depth. Site 3 was too sandy, and the corer could not penetrate the sediment. Sediment was sectioned as 4-cm increments and put into sample bags in the field. These were intended for grain-size and ^{137}Cs analyses. The ^{137}Cs analysis requires more sediment than the ^{210}Pb analysis, which the larger-diameter Russian peat corer provided.

Plexiglass X-radiograph trays were used to collect samples for X-radiography imaging. These trays were 60-cm long. Samples were collected at sites 1, 2, and 4. No core was collected from site 3. These samples were transported back the University of Washington Marine Sciences Building (MSB) intact, and in a vertical orientation, for analysis.

The 15-cm-diameter push core was collected at site 1. This sample was collected for ^{137}Cs analysis after I determined that none of the Russian peat core samples were collected at a sufficient depth for the laboratory analysis. Additional cores were not collected due to safety concerns regarding the +21-cm low-tide level on the field day, expected difficulties with core collection from coarser-grained sites, and the potential for coring to the needed depth of analysis, based on ^{210}Pb accumulation rates. The collection depth below the seabed surface was 55 cm, and the core was transported in a vertical orientation. It was cut in the laboratory into 1-cm-thick sample increments for use in higher-resolution testing than the 4-cm-thick Russian peat core samples would allow.

2.2 Laboratory

Accumulation rates were calculated using ^{210}Pb radiochemistry protocol (Nittrouer et al., 1979). The half-life of ^{210}Pb is 22.3 y, and accumulation rates can be determined for 4-5 half-lives, or ~100 y. Sample increments were chosen to maximize resolution in the upper portions of the cores, but sampling extended over the full lengths of the cores. A maximum of 24 samples can be analyzed at a time, so 12 samples each from sites 1 and 2 were analyzed simultaneously. After analysis, I determined that the core from site 1 did not extend deep enough into the seabed. A second core was collected at the same location and extended to 100 cm. I analyzed 12 samples each from sites 1 and 3. Site 4, the location where I anticipated the greatest accumulation rates, was analyzed to a higher resolution with 24 samples. Alpha-decay counting was conducted using Ortec Ametek and Octete Plus alpha spectrometers.

Data analysis was done in Matlab, based on the following equation (a):

$$A=(\lambda Z)/\ln(D_0-D_z),$$

where λ is the decay constant for ^{210}Pb, D_0 and D_z are two depths on the excess ^{210}Pb decay profile, and Z is the vertical distance between those two depths. When using this equation, I assumed that there is no active mixing occurring in the zone of net sediment accumulation. The surface mixed layer depth, where active mixing is occurring, is not included in the calculation. I determined the surface mixed layer depth visually based on the break in vertical slope of the uppermost data points in the ^{210}Pb decay profiles. Supported levels of ^{210}Pb, which also cannot be used to calculate accumulation rates, were determined by a break in slope of data points near the base of the core.

Accumulation rates using the penetration depth of ^{137}Cs decay were measured to corroborate the accumulation rates obtained using ^{210}Pb (Ritchie, 1970). As a byproduct of global nuclear programs, ^{137}Cs has a distinct time horizon in marine sediments. Significant deposition began in 1954, and peaked in 1963 (Delaune et al., 1978). If a depth of penetration to the 1963 ^{137}Cs peak agrees with the predicted 1963 depth from the ^{210} Pb accumulation rate, then the ^{210}Pb accumulation rate is robust. Samples were weighed, dried and crushed in preparation for gamma-decay counting. Gamma-decay counting was conducted using a Canberra DSA LX signal analyzer with Canberra Genie 2000 spectroscopy software. Data were plotted in Excel to determine the 1963 penetration depth. The penetration depth for 1963 using ^{210}Pb was calculated by multiplying the years since 1963 with the previously calculated accumulation rate, then adding the surface mixed depth.

X-radiography negative images were collected at the MSB, using a Faxitron Torrex cabinet x-ray system. I developed the negatives manually in the dark room of the same building. Digital

scanning of the negatives was done using an Umax Powerlook 2100XL digital scanner. Images were intended to help interpret anomalies in the ^{210}Pb profiles and grain-size distributions.

Grain-size analysis was completed using a Beckman Coulter LS 13 320 laser-diffraction particle-size analyzer at the MSB. I first mixed each sample to homogenize it, and then weighed ~1 g of sediment from each sample collection interval, mixed it with a 0.05% sodium metaphosphate dispersant, and sonicated it for at least 15 minutes. Samples were put through a 0.2-cm sieve prior to analysis to remove any gravel, which the Beckman Coulter cannot analyze. Sieving removed fibrous organics from cores 1, 3 and 4, and gravel and shell material from 4 depth intervals in core 3. The reported data were an average of three consecutively run one-minute grain-size analyses. Distributions were used to determine the general sedimentation trends in the bay over time and to identify anomalies that do not reflect the prevailing trends.

3.0 Results:

3.1 Accumulation rates

^{210}Pb activity in excess of the supported (background) ^{210}Pb value of 0.19 dpm/g was determined for twelve samples in each of cores 1, 2 and 3, and 24 samples at core 4 (Appendix B). I fit a regression line to activity vs. depth plots, omitting a surface mixed layer of 5-20 cm, dependent on site (Fig. 11). Using equation (a), the calculated accumulation rate ranged from 0.20 to 1.07 cm yr^{-1}. Sites 2 and 3, near the center of the bay, show substantially lower accumulation rates (0.23 and 0.20 cm yr^{-1}, respectively) than at sites 1 and 4, on the east side of the bay (0.83 and 1.07 cm yr^{-1}, respectively). Line fits with R^2 ranging from 0.57 to 0.84 suggest that the accumulation process at all sites were relatively steady.

The ^{137}Cs depth of penetration to 1963 was 51.5 cm in core 1, which is similar to the ^{210}Pb predicted penetration depth of 50.6 cm and validates the ^{210}Pb accumulation rates (fig. 12)

(Appendix B). Validation using ^{137}Cs supports my assumption that there is no active mixing below the surface mixed layer.

3.2 Grain-size distributions

Sediment at the coring sites is dominated by silt and very-fine to medium sand. All four sites demonstrate a fining-up trend of the coarse-grained clasts, with very coarse sand present at depth and absent or nearly absent at the surface (fig. 13). Sites 1 and 4 are finer grained than sites 2 and 3. The relative abundance of fine-grained sediment at each site does not show a fining trend. Site 1 contains a coarser anomaly for ~40-60 cm below the bed surface and a spike in the relative abundance of silt at 60-70 cm. Site 2 is nearly uniform, with only a slight reduction in coarse sand at the shallowest samples. Site 3 has a finer anomaly at ~12-14 cm below the bed surface. Site 4 contains finer anomalies at ~16 to 20 cm below the bed surface and again at ~28 to 36 cm below the bed surface, and a strong spike in silt at 70-80 cm depth.

3.3 X-radiograph analysis

The X-radiograph images at site 1 show mottling and homogenization from the ground surface to a depth of ~20 cm. A bivalve and burrow are preserved in this section. From 20 cm to 42 cm depth there is mm-scale to cm-scale bedding with some mottling. Bedding alternates between coarser and finer layers, with an ~1-cm-thick fine layer at 30-cm depth (fig. 14). The site 2 X-radiograph is mottled, with no primary structure preserved. The core contains gravel and shell from ~24-cm depth down. There is a sample collection artifact at ~4-cm depth that does not represent preserved structure (fig. 15). Collecting an X-radiograph tray core at site 3 was not possible due to sandy sediments. X-radiograph images from site 4 reveal mottling, except for a finer feature from ~16-cm to 20-cm depth. There are traces of gravel and shells from 32 cm to the core bottom (fig. 16).

4.0 Discussion:

4.1 Small-scale industry effects

The usefulness of ^{210}Pb for dating, as previously stated, extends back ~100 y. This timeframe makes it difficult to evaluate changes in sedimentation processes prior to 1920. Due to this limitation I cannot say whether the small-scale industrial and residential activities that occurred on or near the bay prior to 1920 had any effect on sediment accumulation. If sediment accumulation rates are accurately represented by the ^{210}Pb analyses and are constant through time, the grain-size distributions curves from sites 1, 2 and 3 extend to accumulation depths before 1920. At site 1, the depth to 1920 should be approximately within the depth interval 80 to 90 cm; at site 2, the 1920 depth should be at 20 to 24 cm; at Site 3, the 1920 depth should be at 18 to 20 cm. At site 3 there is an ~10% increase in relative abundance of fines at this depth. All three sites show a >5% increase in relative abundance of fines at depths 70 to 80 cm, 16 to 20 cm, and 16 to 18 cm respectively, which still fit within the 1920s construction timeframe. In other locations, causeway construction has been linked to rapid changes in sedimentation both during, and in the immediate years proceeding, completion (Proosdij et al., 2009). This fining I observe during the 1920s may indicate an effect of the causeway on grain size deposited in the Mud Bay.

4.2 Causeway effects on accumulation rates

Based on the ^{210}Pb profiles showing constant accumulation rates, I cannot definitively state that construction of the causeway has resulted in an increase of sediment accumulation in Mud Bay. If accumulation rates changed, I would expect to see changes of slope in the logarithmic-decay profiles, which are not observed. Except in the case of site 4, these decay profiles were based on limited data points, excluding the surface mixed layer and supported ^{210}Pb points. Higher-resolution ^{210}Pb analysis could be done on these sites to better constrain any changes of slope in the decay profiles.

4.3 Interstate 5 effects on accumulation rates

Any increased accumulation rates related to Interstate 5 are likely constrained to short-term events, limited to the time-period of construction. There are anomalies in the grain-size distributions at three sites that could contain an Interstate 5 signature. Assuming peak impact around 1963 during construction grading, elapsed time between then and sampling is about 55 years This estimate is variable as construction was completed over a period of about 11 years, ending in 1966 (Hillegas, 2004). Using these dates and ^{210}Pb-determined accumulation rates, I estimated the depth at which construction-related sediments might occur in each core. At site 1, this corresponds to ~45 cm dept within an interval of coarsening located from 40 to 60 cm. As this site was located closest to the creek mouth, this is where coarser bedload particles would be expected to deposit as the creek gradient shallows and transport capacity lessens. At sites 3 and 4, there are fining anomalies at 12 to 14 cm and at 60 to 65 cm, respectively. These depths also correspond roughly with Interstate 5 construction, and I interpret these anomalies as the finer of the coarse-grained bedload sediments and suspended silts that were deposited distal from the creek mouth.

Chuckanut Creek does flood, but there are no stream-gauge data prior to 2005 or historic flood records, and no nearby comparable proxy. Using the limited COB Arroyo Park stream-gauge discharge data, the average daily discharge of Chuckanut Creek is ~0.4 cubic meters per second (cms). On 1/7/2009 and 1/8/2009, the daily discharges were ~34 cms and 19 cms respectively, at least two times greater than the next-largest daily discharge for the 2009 water year. Stream gauge data were provided by Michelle Evans of the COB Public Works Office (personal communication, 2019). A daily discharge of 34 cms represents a 10-year event (COB, 2016). The National Oceanic and Atmospheric Administration (NOAA) precipitation records show that there was a cumulative rainfall of ~7.5 cm for 1/6/2009 and 1/7/2009 (2019 a). Using this rough correlation, I assume that 2 consecutive days of ≥7.5 cm of precipitation represent a flood event.

Under this assumption, there were 13 flood events between 1920 and 2019, using 97% complete precipitation data (NOAA, 2019 a and b). This includes a potential flood event in 1958 that could also explain the sedimentation anomalies seen during Interstate 5 construction (NOAA, 2019 b). The site-4 fine-sediment anomaly seen from 70 to 80 cm could be the result of flood events in 1945 and 1949

4.4 Spatial patterns in grain size

As noted above, grain size varies systematically at the four coring sites. Sediment is entering Mud Bay from the creek and slope wash from the surrounding hillsides, and in suspension from the incoming tide. This should result in the finer sediments being found towards the center of the bay, where you would expect deeper bathymetry and less wave interaction with the seabed. In Mud Bay, the opposite is happening, evidenced by the finer-grained sites located closer to the shore on the east side of the bay. I interpret this to be due to a change in the energy dynamic due to the causeway, which is essentially acting as an artificial barrier coastline, evidenced by the development of a flood-tide delta in the bay (fig. 9). Fines now depositing at sites 1 and 4 would have been subject to greater tidal and wave energy, as well as energy from the tidal channels, prior to the causeway construction. Because the causeway shelters the shore, these energies no longer resuspend and transport fines out of the east side of the bay, and the center of the bay, located near the causeway opening, is now the higher-energy environment. The erosional features on the west side of the bay give evidence that the shoreline previously had a higher energy environment than seen today.

4.5 Spatial patterns in accumulation rates

Spatial patterns in the accumulation rates also correspond to the anticipated energy at each site. Sites 2 and 3, with lower accumulation rates, are both located closer to the causeway opening and they are at about the same elevation as the tidal channel. More sediment can be resuspended and transported by both tidal and fluvial means at these locations. There is little or

no fining-up trend observed at site 2, implying that this site could be most indicative of pre-causeway bay conditions. This site is closest to the causeway opening, ~300 m behind the causeway, and it is likely that it would receive more tidal energy than the other sites. The two sites 1 and 4, located more distally from the opening, and elevated above the creek and tidal channels, have the greatest accumulation rates. My interpretation of these spatial variations in accumulation rates is that sites 1 and 4 are in a more quiescent area of the bay, which corroborates the changed energy distribution discussed in section 4.4. An additional opening in the causeway to the east could increase tidal flushing and remove some of this sediment.

4.6 Sea-level rise to date

Sea level has been rising over the time period covered in this study. The magnitude of sea-level rise will affect how much the bay has filled with sediment, if at all. According to NOAA, sea level has risen in the Bellingham area by an average of 0.12 ±0.027 cm yr^{-1} since 1934, when data collection began (2018). This is based on data collected from NOAA tide gauge 9449880, located in Friday Harbor, Washington. Friday Harbor was chosen as a proxy for Mud Bay due to both locations still undergoing isostatic rebound at a rate of ~0.03 mm yr^{-1} (Washington Coastal Hazards Resilience Network, 2018), and having similar semi-diurnal mesotidal cycles. NOAA has not calculated historical sea-level rise for Bellingham or Chuckanut Bay.

4.7 Magnitude of Mud Bay infilling

Sediment accumulation rates in Mud Bay range from 0.20 cm yr^{-1} to 1.07 cm yr^{-1}. To put that into context, those accumulation rates compare to those of the Skagit River delta, which range from 0.16-1.04 cm yr^{-1} (Webster, 2013). Near Mount Vernon, the Skagit River discharges a mean of 2.5 million metric tons of suspended sediment annually, accounting for 40% of sediment transported into Puget Sound (Curran, 2016) and dwarfing sediment supply by Chuckanut Creek. Given that sea level has risen by 0.12 cm yr^{-1}, the bay has filled with sediment for at least 85 years at a rate greater than sea-level rise at my coring sites.

4.8 Relative sea-level-rise projections

There is the potential for future sea-level rise to outpace sediment accumulation in Mud Bay. If so, the negative effects of incoming sediment could be minor to nonexistent. There is variability in the estimated rate of relative sea-level rise. The Washington Coastal Network report (2018) gives estimates for both low and high greenhouse gas scenarios, RCP 4.5 and RCP 8.5 respectively. The RCP greenhouse gas concentration pathways are the metrics currently use by the Intergovernmental Panel on Climate Change for modeling, with RCP 8.5 representing the worst-case scenario. At a 50% probability of exceedance for each RCP the projected relative sea-level rise at Mud Bay ranges from 0.55 cm yr^{-1} to 0.71 cm yr^{-1} by 2100. These rates take isostatic rebound into account. I also used Mazzotti et al. (2008), who implemented tide-gauge and GPS data to estimate vertical land changes. They predict a relative sea-level rise rate of ~0.38 cm yr^{-1} by 2100. I can reasonably expect sea level to rise somewhere between ~0.38 cm yr^{-1} to 0.71 cm yr^{-1} by 2100.

4.9 Future projections for Mud Bay infilling

Given an estimated relative sea-level rise of ~0.38 to 0.71 cm yr^{-1} (Mazzotti et al., 2007, Washington Coastal Hazards Resilience Network, 2018), and assuming that sediment accumulation rates remain constant, the east side of the bay where sites 1 and 4 are located will continue to fill with sediment. The center of the bay, where sites 2 and 3 are located, will not continue to fill under the same assumption. The spatial distribution of accumulation rates supports the hypothesis that proximity to the causeway opening is a factor in sedimentation patterns, and that adding another opening in the causeway to the east could increase tidal flushing and reduce accumulation at sites 1 and 4.

4.10 X-radiography analysis

X-radiograph images do not show much sedimentary structure. The high degree of bioturbation validates my use of ^{137}CS to ensure that mixing was contained to the surface mixed layer. There

are centimeter-scale structures preserved in cores for sites 1 and 4 that could be signatures of flood events. The bedding at site 1 is at ~30-cm depth. Assuming the accumulation rate of 0.83 cm yr^{-1} calculated for this site, that depth correlates with 1982. On 2/13/1982 and 2/14/1982 there were daily rainfalls of ~6.2 cm and 4.2 cm respectively (NOAA, 2019 a). Using my above described flood proxy method, I interpret that this bedding structure most likely records a flood event. The fine-grained bedding in the site 4 X-radiograph seen at the 16 cm to 20 cm depth correlates with 1998. The precipitation data is missing from the NOAA records from January through August of that year, so I cannot validate that this is a flood event, though that is the most likely interpretation. The X-radiograph data are limited by the length of the collection trays, and these images do not extend beyond 46 cm below the seabed surface.

4.11 Recommendation for additional work

In general, the lack of previous research in the bay made this study difficult. I had no prior data regarding the best places to core, or how long those cores should be. Additional work in the bay, using results from this study as a guide, could address unanswered questions about anthropogenic effects on the bay. Our understanding of how the environment has reacted to anthropogenic changes helps determine which modifications to the causeway would bring about the most beneficial changes to sedimentation patterns in Mud Bay.

It is possible to better constrain whether grain-size anomalies correlate with Interstate 5 construction. The freeway was built through Chuckanut Formation sandstone, which has a different lithology to the glacial drift found in the creek valley. It is reasonable to infer that if Chuckanut Creek carried sediment derived from construction, then point counts of sediment accumulated during construction would differ from sediment derived from more typical erosional processes (Wratten, 2019). These point counts could be used to evaluate an Interstate

5 signature. In addition, calculating transport capacity and sediment flux for Chuckanut Creek would help determine how much sediment is entering the bay from the primary fluvial source.

A greater distribution of grain-size analyses could help constrain the energy distribution within Mud Bay, and where a new causeway opening might be the most beneficial. Using my accumulation rates as a guide, it would be possible to conduct multiple grain-size distributions on cores representative of >100 years to better determine changes in sedimentation prior to and after the causeway was built, particularly on the east side of the bay.

Better constraining how much bedload and suspended sediment Chuckanut Creek transports into the bay would help answer questions about how rapidly the bay will continue filling. A sediment budget could be built for Chuckanut Creek using both field data and modeling.

I would recommend that future coring in the bay be done using vibracoring methods. This would allow for conducting higher-resolution ^{210}Pb analysis to constrain any changes of slope in the regression that could indicate a change in accumulation rate. X-radiography could also be conducted at deeper depths, and at coarser-grained locations, with a vibracore.

5.0 Conclusions

Mud Bay is an important natural habitat that has been identified as a top-priority restoration site due to high levels of sediment accumulation leading to habitat degradation. Multiple anthropogenic modifications and activities could have caused increased sediment accumulation rates, the most notable are the building of the railroad causeway in the 1920s and the construction of Interstate 5 in the 1960s. There is evidence of a flipped energy distribution in the bay that could be related to changes in tidal-energy distribution after the causeway was constructed. Short-term increase in relative proportions of silt at the depth consistent with the age of Interstate 5 construction suggest that this event is also recorded in the bay sediment. The

bay has been filling with sediment at a rate greater than sea-level rise since 1934. A comparison of accumulation rates to projected relative sea-level rise in the bay indicates that the east side of Mud Bay will continue infilling with sediment. The proposal put forth by the City of Bellingham to modify the causeway and allow for more tidal and wave flushing in the bay might alleviate the present sediment conditions, but more work should be done in the area to define unknown variables, get a better understanding of the effects of opening the causeway, and help determine where a new opening would have the greatest positive effects.

References:

Boldt, K.V.; Nittrouer, C.A.; and Ogston, A.S., 2013, Seasonal transfer and net accumulation of fine sediment on a muddy tide flat: Willapa Bay, WA: *Continental Shelf Research*, Vol. 60, pp. s157-s172.

Davis, D. H., 1993, *Log Chutes on the Industrial Frontier: A case Study of Chuckanut Mountain, Whatcom County, Washington*: Unpublished M.A. Thesis, Department of Anthropology, Western Washington University, Bellingham, WA., 199 p.

Delaune, R.D.; Patrick, W. H. Jr.; and Buresh, R. J., 1978, Sedimentation rates determined by ^{137}Cs dating in a rapidly accreting salt marsh: *Nature*, Vol. 275, pp. 532-533.

City of Bellingham, 2011, *City of Bellingham shoreline characterizations Chuckanut Creek SMA*: Electronic document, available at https://www.cob.org/Documents/planning/environments/smp/characterizations-inventory/chuckanut-text-summary.pdf

City of Bellingham, 2011, *City of Bellingham shoreline characterizations Marine SMA*: Electronic document, available at http://www.cob.org/Documents/planning/environments/smp/characterizations-inventory/marine-text-summary.pdf

City of Bellingham, 2019, *City IQ 2017 FEMA flood-zone map*: Electronic document, available at https://www.iqmap.org/geviewer/Html5Viewer/Index.html?viewer=cityiq

City of Bellingham Department of Public Works, 2006, *Urban stream monitoring report 2006*: Electronic document, available at https://www.cob.org/Documents/pw/environments/2006-urban-streams-monitoring-report.pdf

City of Bellingham Department of Public Works Laboratory, 2016, *Urban stream monitoring report 2015*: Electronic document, available at https://www.cob.org/Documents/pw/environments/2015-urban-streams-monitoring-report.pdf

Curran, C. A., Grossman, E. E., Mastin, M. C. and Huffman, R. L., 2016, *Sediment load and distribution in the lower Skagit River, Skagit County, Washington*: U.S. Geological Survey Scientific Investigations Report 2016-5106, 34 p.

Easterbrook, D. J., 1976, *Geologic map of western Whatcom County*: U.S. Geological Survey map, scale 1:62,500, 1 sheet.

Eissinger, A., 1995, *City of Bellingham wildlife and habitat assessment, and inventory of existing conditions and background information, and wildlife habitat plan*: Electronic document, available at https://www.cob.org/Documents/planning/growth/fairhaven_high/wildlife-habitat-assessment.pdf

Eissinger, A., 2003, *City of Bellingham wildlife habitat assessment*: Electronic document, available at https://www.cob.org/Documents/pw/environments/restoration/wildlife-habitat-assessment-2003.pdf

Evans, M., 2019, personal communication, water quality specialist, Public Works, City of Bellingham, 2221 Pacific Street, Bellingham, WA, 98229.

Farrow, L., Garrett, J., Langton, J., Olsen, S., Parsons, J., Pfaff, B., Sakshian,, R., and Van Doornik, D., 1989, *Chuckanut Village environmental impact study*: Unpublished course project, Huxley College of Environmental Studies, Western Washington University, Bellingham, WA, 73 p.

Gerner, W., 2017, personal communication, Chuckanut Village resident, 3615 18th St., Bellingham, WA., 98229-9348.

Hillegas, J. V., 2004, "Pushing forward with the determination of the machine age": Interstate 5 is built through Bellingham, Washington, 1945-1966: *Journal Whatcom County Historical Society,* special edition Bellingham centennial, pp. 105-138.

Johnson, S. Y., 1982, *Stratigraphy, Sedimentology, and Tectonic Setting of the Eocene Chuckanut Formation, Northwest Washington: Unpublished PhD Dissertation, Department of Geological Sciences, University of Washington, Seattle, WA., 400 p.*

Lewis, H. B., and Alberton, C. H., 1891, *Plat showing streets of the city of Fairhaven produced to the harbor line and showing the location of railroad avenue within the city limits,* scale 1:4,800: Electronic document, available at https://docs.cob.org/PublicAccess/PublicAccessProvider.ashx?action=ViewDcument&overlay+Print&overrideformat=PDF

MacLennan, A., Schlenger, P., Williams, S., Johannessen, J., and Wilkinson, H., January 2013, *WRIA 1, nearshore and estuarine assessment and restoration prioritization*: Electronic document, available at https://cob.org/documents/pw/environment/restoration/master-plan/wria1-nearp-report.pdf

MacLennan, A., Williams, S., and Johannessen, J., December 2013, *WRIA 1 nearshore and estuarine assessment and restoration prioritization-addendum 1*: Electronic document, available at https://www.cob.org/wria1-nearshore-estuarine-assessment-restoration-prioritization-addendum-2014.pdf

Mazzotti, S., Jones, C., and Thomson, R. E., 2008, Relative and absolute sea level rise in Western Canada and northwestern United States from a combined tide gauge-GPS analysis: *Journal Geophysical Research*, Vol. 113, C11019.

Miller, D., 2019, personal communication, Chuckanut Village resident, 3605 19th St., Bellingham, WA., 98229-9347.

Miller, J., 2017, personal communication, Chuckanut Village resident, 3605 19th St., Bellingham, WA., 98229-9347.

Mullineaux, D. R., Waldron, H. H., and Rubin, M., 1965, *Stratigraphy and chronology of late interglacial and early Vashon glacial time in the Seattle area, Washington*: U.S. Geological Survey Bulletin 1194-0, 10 p.

National Oceanic and Atmospheric Administration, 2018, *U.S. linear relative sea level rise (RSL) trends and 95% confidence intervals (CI) in mm/year and ft/century*: Electronic document, available at https://tidesandcurrents.noaa.gov/sltrends/msiUSTrendsTable.html

National Oceanic and Atmospheric Administration, 2019, *Daily summaries station details GHCND:USC00450564*: Electronic document, available at https://www.ncdc.noaa.gov/cdo-web/datasets/GHCND/stations/GHCND:USC00450564/detail

National Oceanic and Atmospheric Administration, 2019, *Daily summaries station detail GHCND:USC00450569*: Electronic document, available at https://www.ncdc.noaa.gov/cdo-web/datasets/GHCND/stations/GHCND:USC00450569/detail

Nittrouer, C. A., Sternberg, R. W., Carpenter, R., and Bennett, J. T., 1979, The use of Pb-210 geochronology as a sedimentological tool: application to the Washington continental shelf: *Marine Geology,* Vol. 31, pp. 296-316.

Northwest Ecological Services, LLC., 2006, *Management recommendations for the city of Bellingham pocket estuaries*: Electronic document, available at https://www.cob.org?Documents/pw/environments/restoration/pocket-estuary-mgmt-recommendations-02.06.pdf

Pritchett, H. S., 1898, *Bellingham Bay, Washington*: U.S. Coast and Geodetic Survey Navigation Chart, Plate 2460, scale 1:40,000, 1 sheet.

van Proosdij, D., Milligan, T., Bugden, G., and Butler, K., 2009, A tale of two macro tidal estuaries: differential morphodynamic response of the intertidal zone to causeway construction: *Journal of Coastal Research,* Vol. 1, pp. 772-776.

Thomas, R. B., 1971, *Chuckanut Chronicals*: Chuckanut Fire District Auxiliary, Bellingham, WA., 64 p.

Ritchie, J., 1970, The use of fallout cesium-137 as a tracer of sediment movement and deposition: *Proceedings Water Resources Conference.* Mississippi State University Water Resources Research Institute, Starkville, MS., pp. 149-162.

Ted S. Gacek & Associates, 1984, *Final Environmental Impact Statement Chuckanut Bay Subdivision, Bellingham, Washington:* City of Bellingham Office of Planning and Development, Bellingham, WA., 77 p.

Wahl, T., 2008, *The BNSF railway causeway & its potential modification*: Electronic document, available at https://www.cob.org/Documents/parks/development/projects/woodstock-charrette/4.2-bnsfrw-causeway-potential-modifications.pdf

Washington Coastal Hazards Resilience Project, 2018, *Relative sea level projections for the coastal area near: 48.7N, 122.5W*: Electronic document, available at http://www.wacoastalnetwork.com/files/theme/wcrp/mapdata/RSLProjections_Lat48.7N_Long122.4W.xlsx

Webster, K. L., 2013, *Sediment Dispersal and Accumulation in an Insular Sea: Deltas of Puget Sound*: Unpublished PhD Dissertation, School of Oceanography, University of Washington, Seattle, WA., 159 p.

Wratten, E., 2019, *Sediment Characteristics at the Delta of Chuckanut Creek, Mud Bay, Bellingham, Washington*: Unpublished M.S. Capstone paper, Department of Earth and Space Sciences, University of Washington, Seattle, WA., 50 p.

Figure 1: Aerial image of Mud Bay with study area denoted by the yellow rectangle. Information obtained from Google Earth. Inset shows the location of the bay denoted by the blue star, in reference to Bellingham, WA. Map from the Washington Department of Natural Resources Geology Portal.

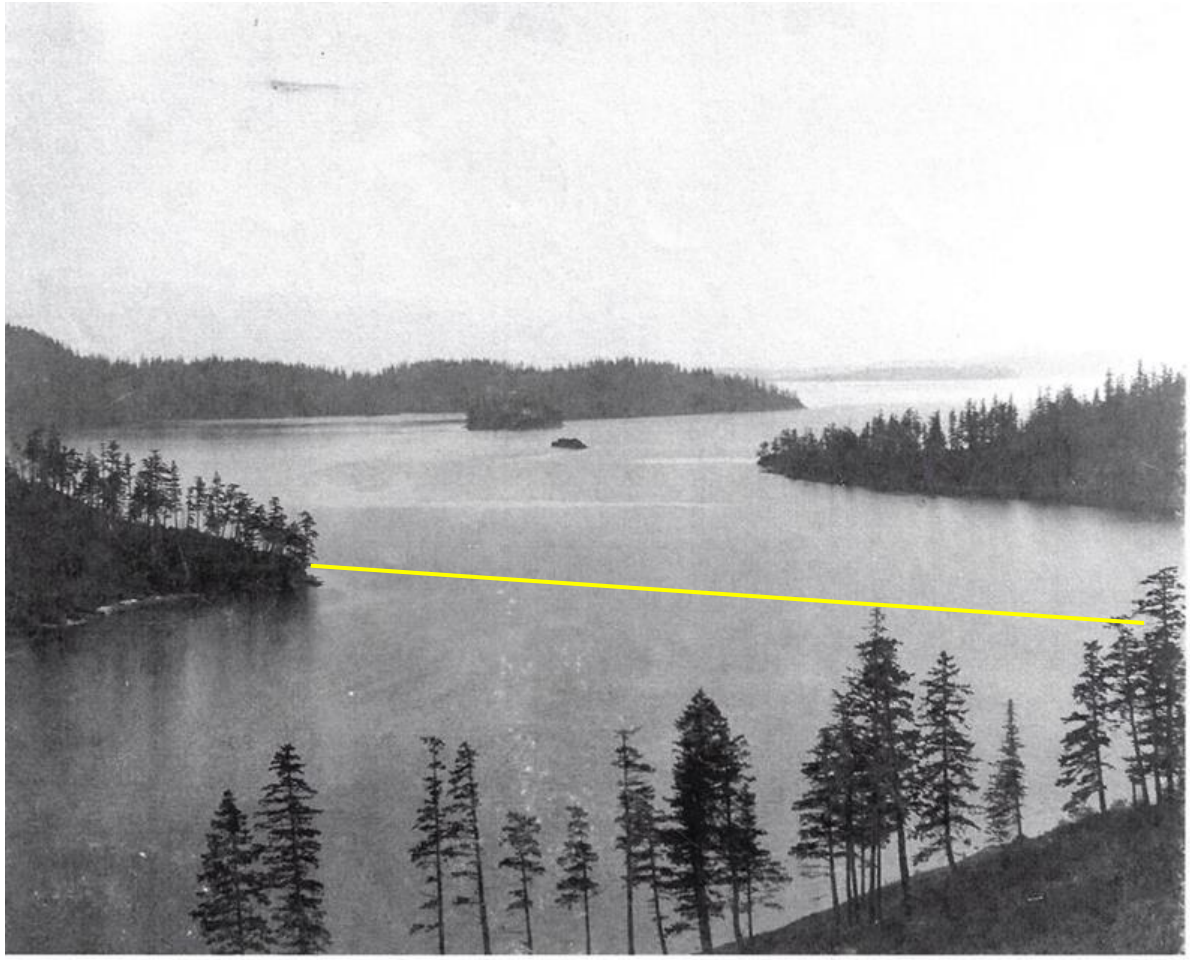

Figure 2: South-facing Late 1800s photograph of Mud Bay, looking towards the bay mouth. The yellow line indicates the natural bathymetric break just seaward of where the railway was built. Image courtesy of the Whatcom Museum.

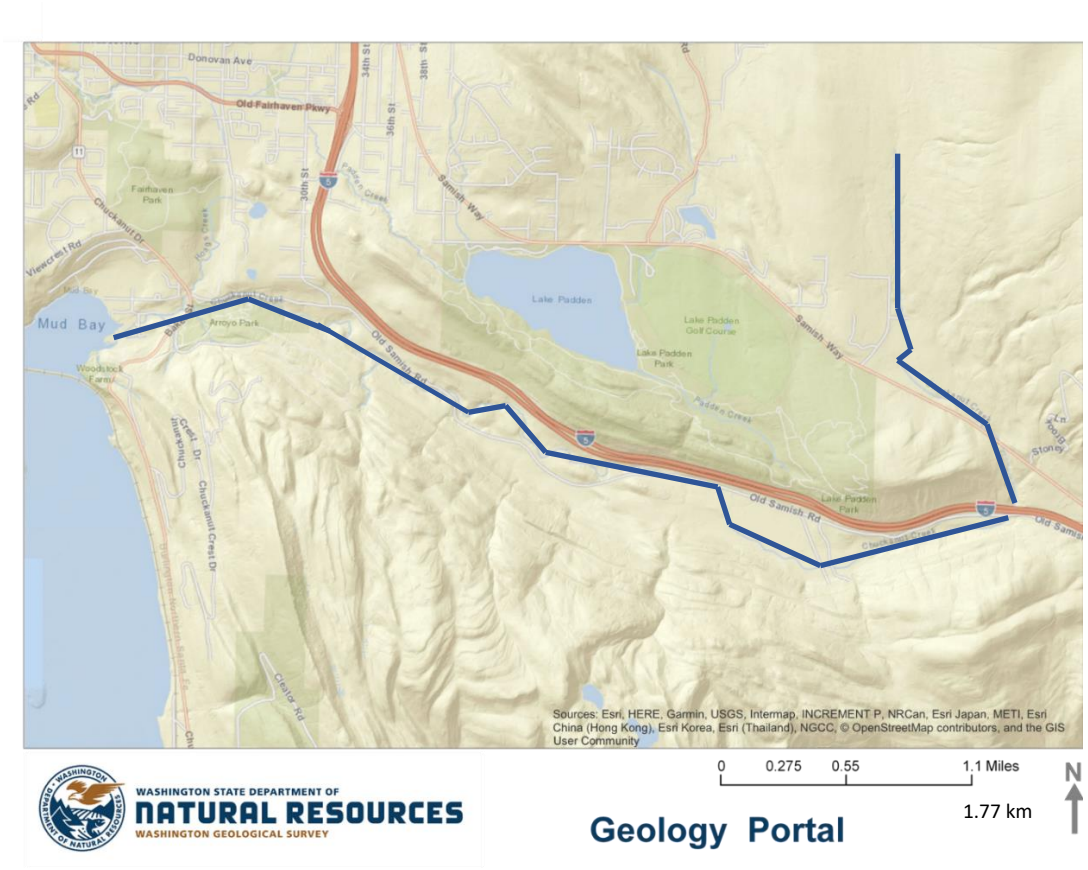

Figure 3: Map showing Chuckanut Creek, approximated by the blue line. Note the proximity to Interstate 5. Map from the Washington Department of Natural Resources Geology Portal.

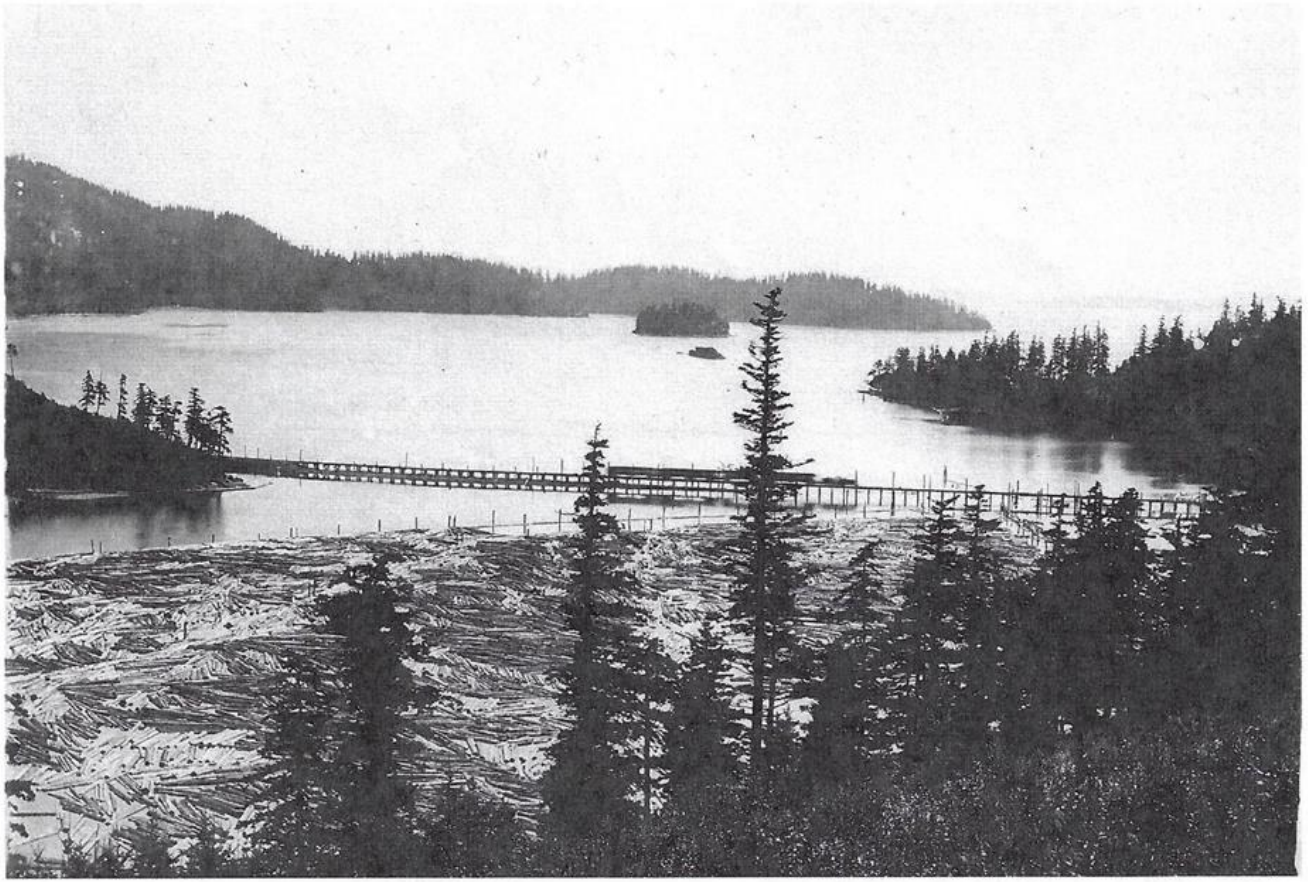

Figure 4: South-facing photograph of the open trestle, completed in 1904. This image also shows the earliest evidence of log-boom storage found for this project. Image courtesy of the Whatcom Museum.

Figure 5: East-facing photograph of Mud Bay with the causeway in the lower right corner, and the position of the 69-m-wide opening indicated with a yellow arrow. The date of this image is unknown, but it was taken after 1920 based on the causeway in the photograph, and is the latest evidence of log-boom storage found for this project. Image courtesy of the Whatcom Museum.

Figure 6: Northwest-facing photograph of the 1920s causeway. Note that this causeway effectively blocks the mouth of the bay. Image taken by Jack Carver, date unknown, and provided courtesy of the Whatcom Museum.

Figure 7: Erosional features in Chuckanut Formation boulders in the northwest side of Mud Bay. These features are indicative of a higher-energy environment than is currently found in the bay. Scout, our 28-kilogram lab assistant, for scale.

Figure 8: Southeast-facing photograph showing loose sediment production during the Interstate 5 construction. Chuckanut Creek location and drainage direction are indicated by the yellow arrow. Image taken by Jack Carver around 1963 and provided courtesy of the Whatcom Museum.

Figure 9: Aerial image showing core locations. Note the sediment plume seaward at the causeway opening, indicative that some sediment leaves the bay. The blue arrow shows a flood-tide delta, indicative of a barrier island coastline analog. Base image from Google Earth.

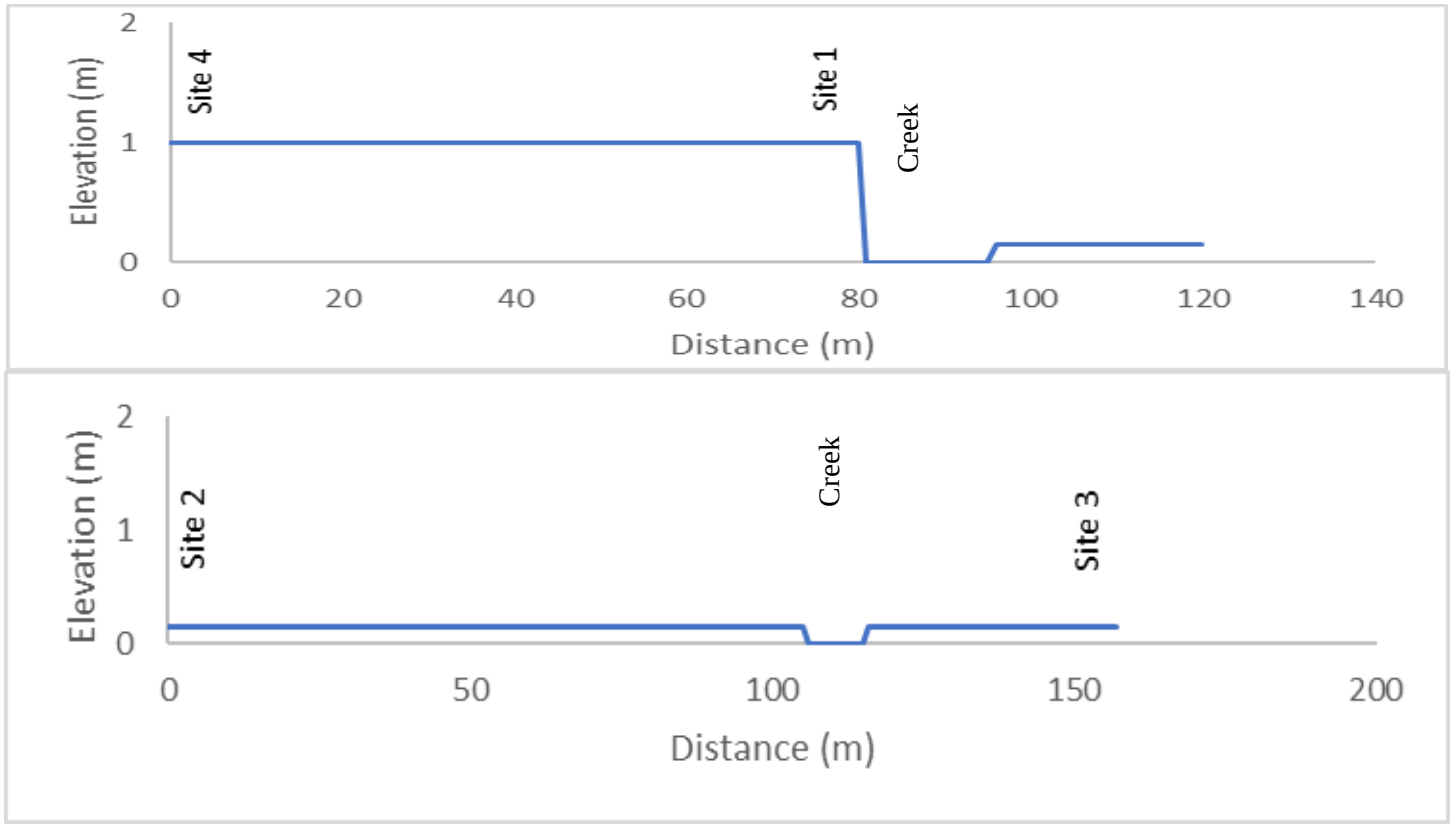

Figure 10: Simplified cross sections indicating relative elevation of coring sites with respect to Chuckanut Creek.

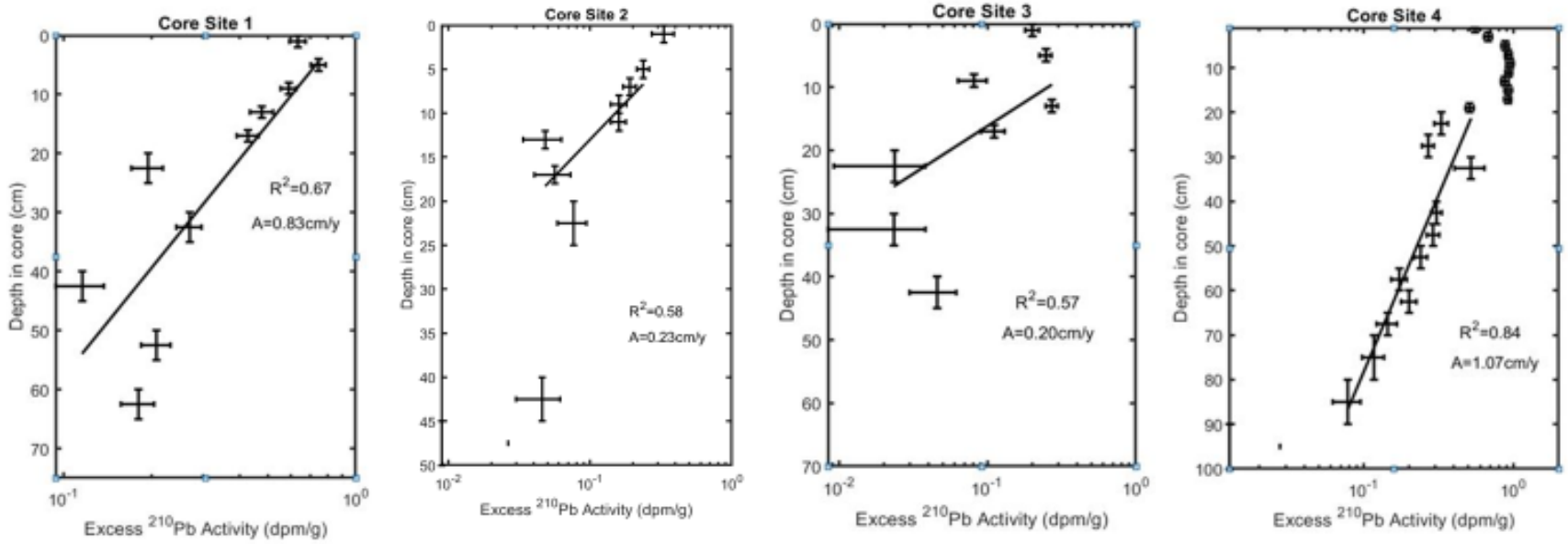

Figure 11: Excess-^{210}Pb profiles showing steady-state accumulation rates. Cores 1, 2 and 3 were collected at depths representing >100 y accumulation, based on the observed accumulation rates. Core 4 does not extend to supported ^{210}Pb depth.

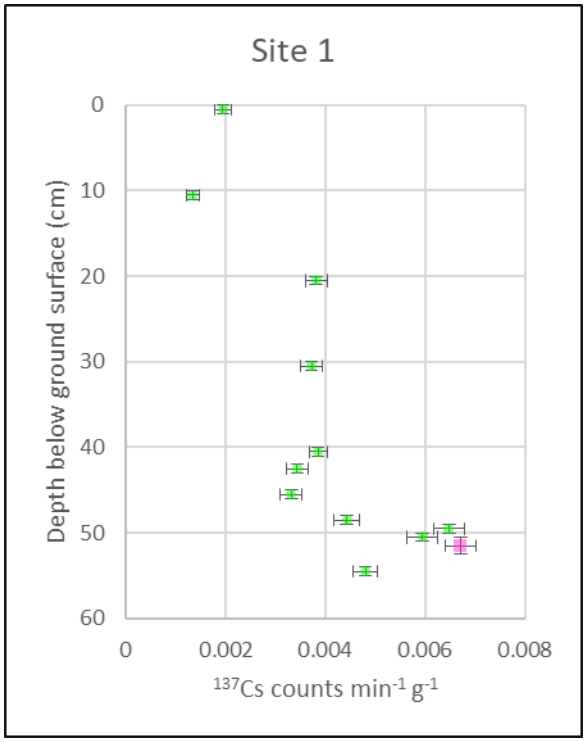

Figure 12 ^{137}Cs-activity graph for site 1 showing the 1963 Cs spike at approximately 51 cm, shown in pink above. This depth agrees with the location of 1963 as calculated using the accumulation rates from ^{210}Pb geochronology, shown in figure 11.

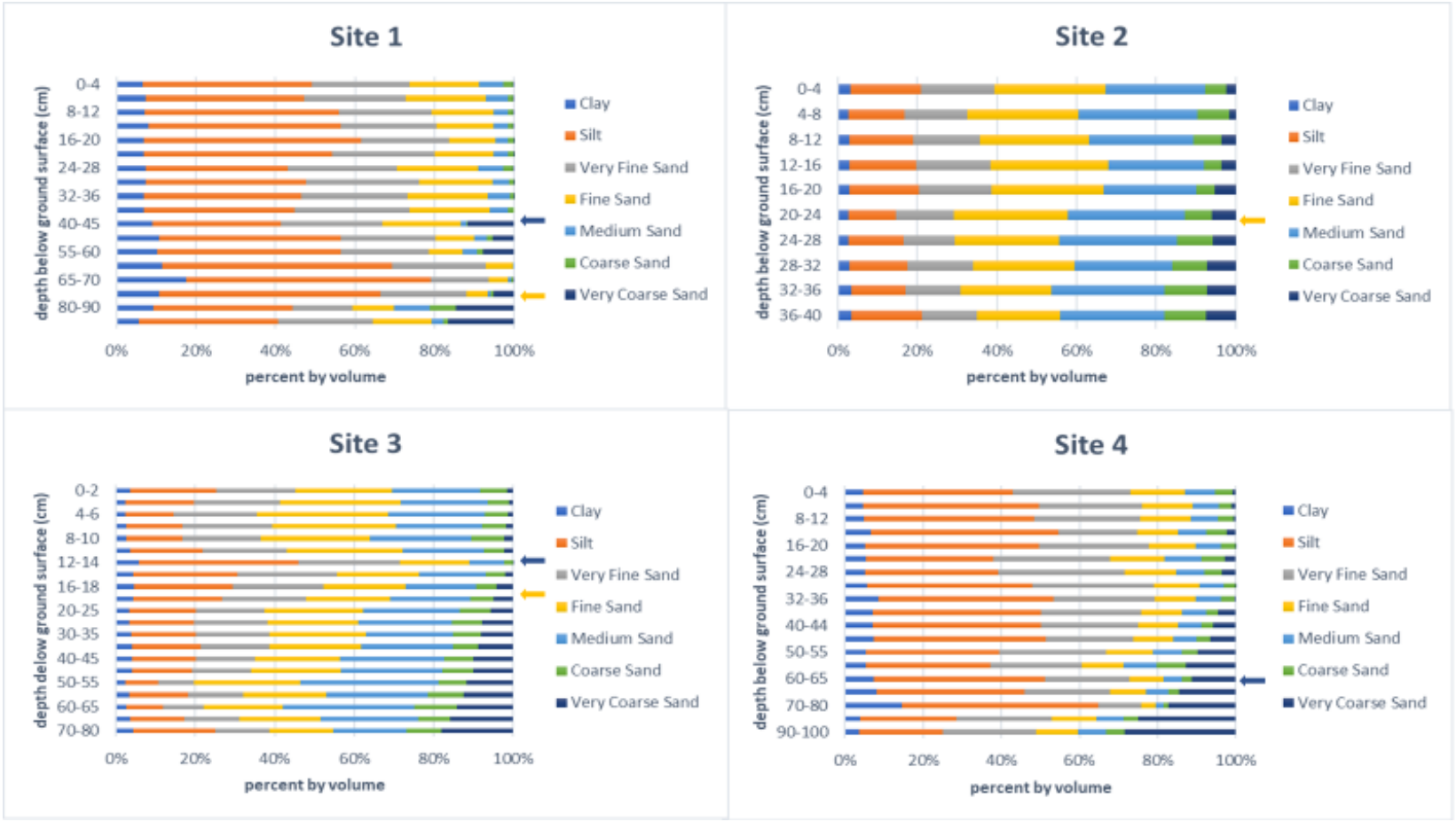

Figure 13 Grain-size distribution plots of the four coring locations. The approximate depth that corresponds to Interstate 5 construction is indicated by a blue arrow, located to the right of each plot. The approximate depth that corresponds to causeway construction is indicated by a yellow arrow. Samples collected at site 4 did not extend far enough beneath the surface to contain the causeway construction depth.

.

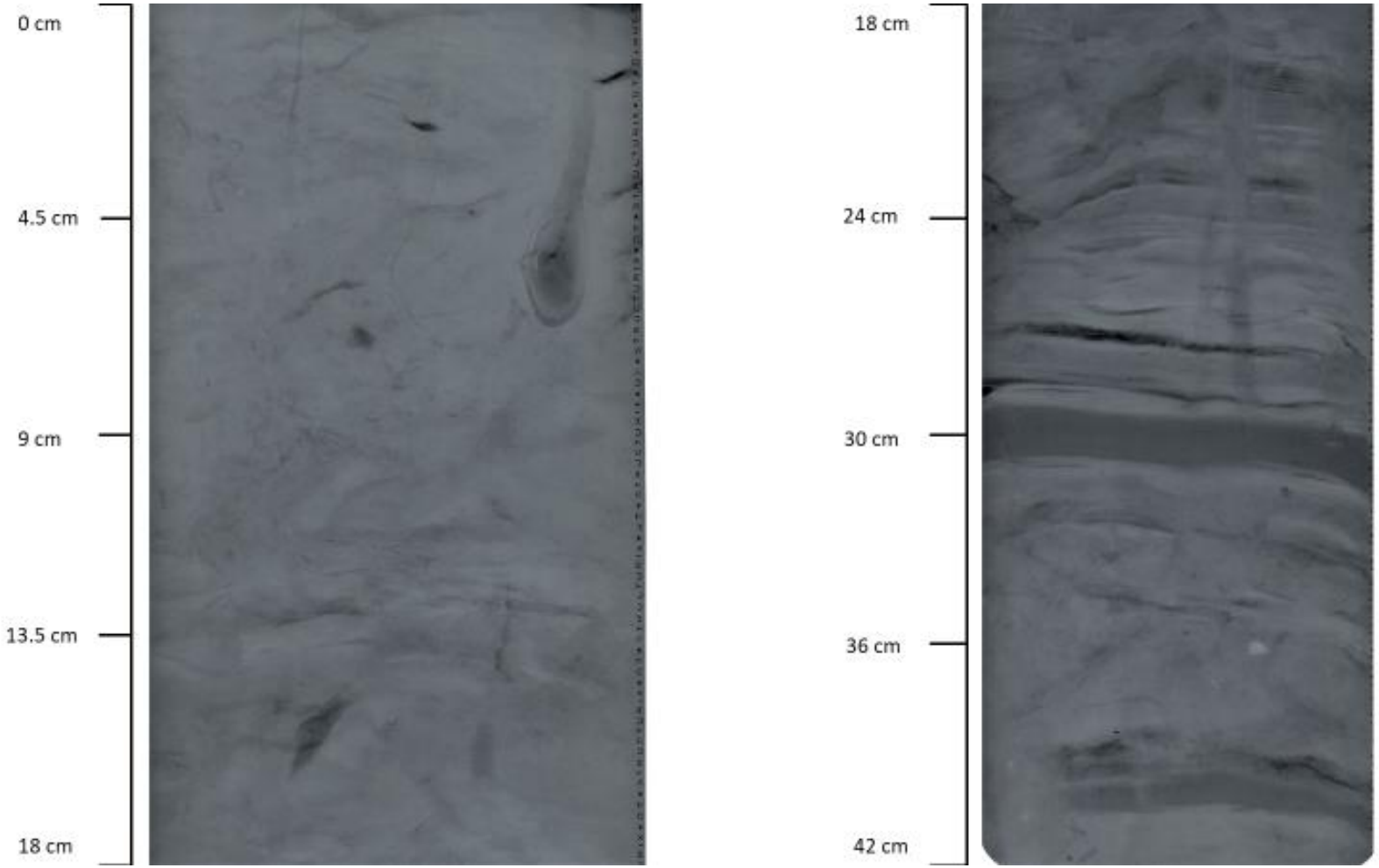

Figure 14: X-radiograph images showing sediment structure at site 1. All images are negatives, with color gradation ranging from black to white as grain sizes increase. Site 1 is mottled or homogenized to ~20-cm depth. Physical structure is mostly preserved from 20 to 30 cm depth and then mottled to 42-cm depth. There is a fine-sediment bedding structure at ~30 cm could be indicative of a flood event in ~1982. Note the bivalve and burrow located ~6 cm below the bed surface.

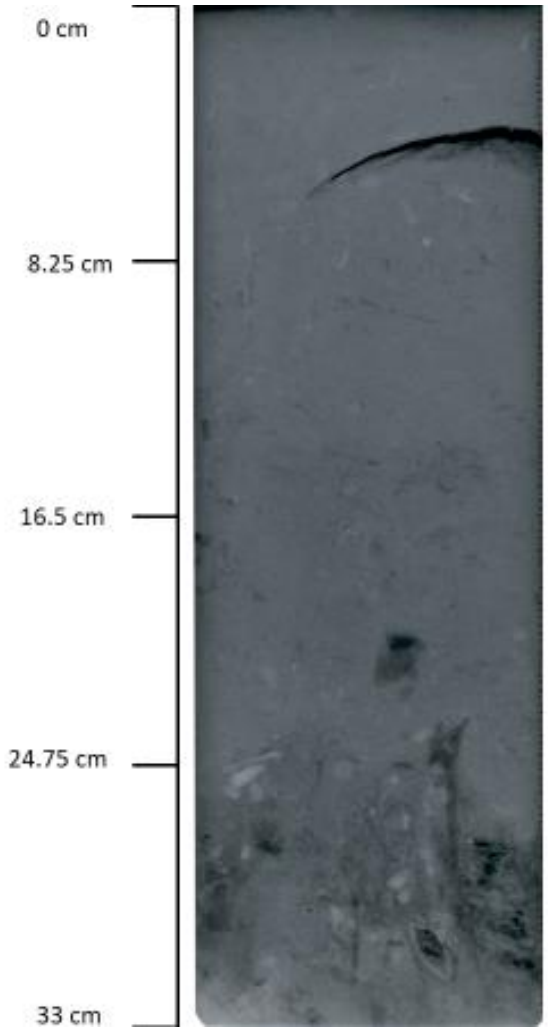

Figure 15: X-radiograph negative image of site 2. There is no primary structure preserved in this image. The dark structure located ~4 cm from the bed surface is an artifact of collection, and does not represent bedding. Below ~24 cm there are coarser sand and shell fragments.

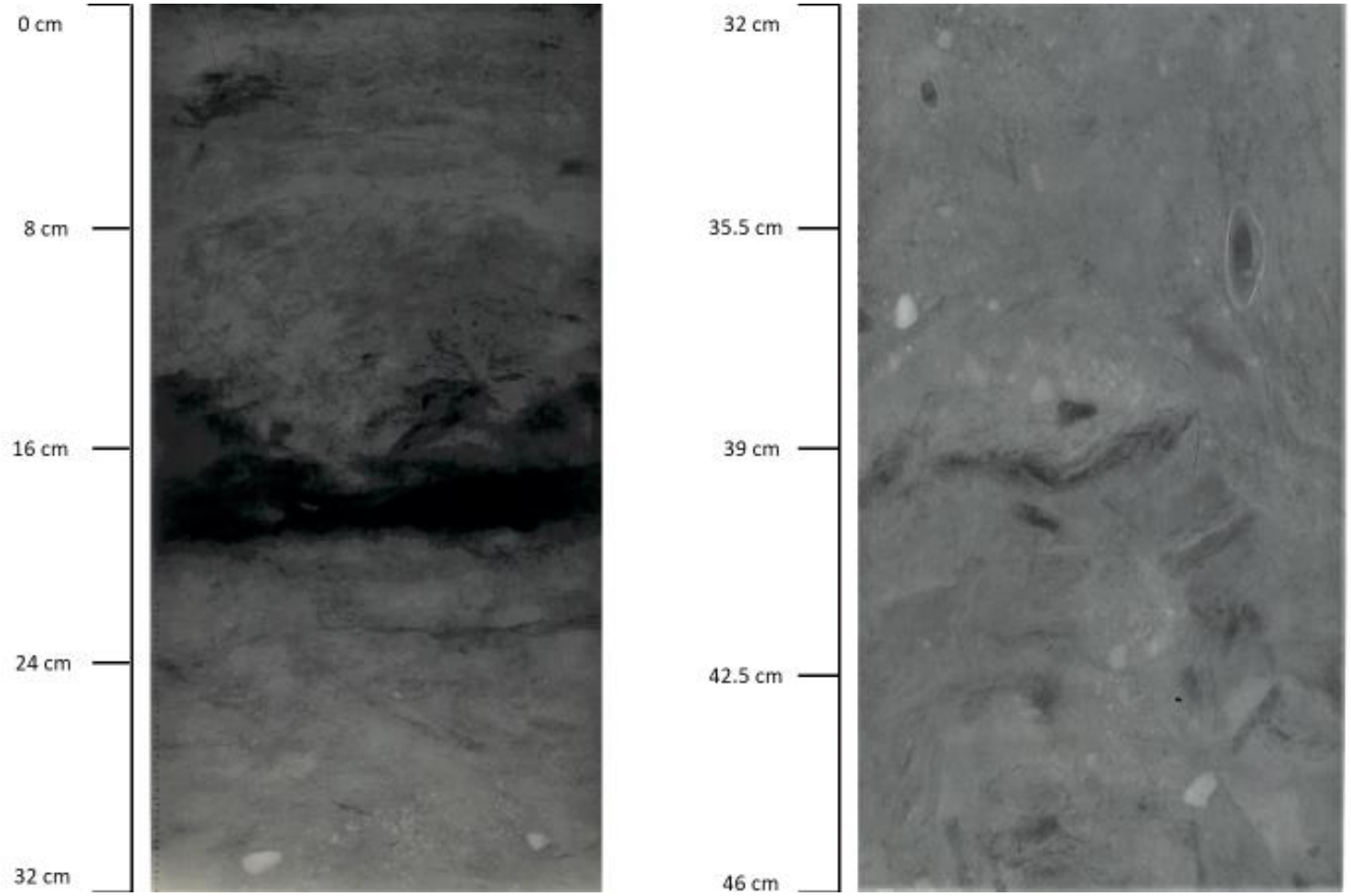

Figure 16: X-radiograph negative images of site 4 is distinctly mottled, with almost no primary structure preserved. There is a finer-grained bedding structure located from ~16 to 20 cm depth that could be indicative of a flood event in ~1998.

Appendix A - Core data

Site	Latitude	Longitude	Core type	Depth (cm)	Date collected	Low tide height (cm)
1	48.699291	-122.498359	GC	50	5/4/2018	-17
			RP	50	5/4/2018	-17
			X-R	42	5/4/2018	-17
			GC	90	6/28/2018	-47.5
			15 cm	55	10/22/2018	+21
2	48.699428	-122.50172	GC	50	5/4/2018	-17
			RP	50	5/4/2018	-17
			X-R	33	5/4/2018	-17
3	48.700375	-122.500139	GC	80	6/28/2018	-47.5
4	48.699225	-122.499439	GC	100	6/28/2018	-47.5
			RP	50	6/28/2018	-47.5
			X-R	46	6/28/2018	-47.5

Appendix B – Radiochemical data

Site	Depth interval (cm)	Alpha Counter	^{210}Pb activity	Depth plotted (cm)	Horizontal error (±)	Vertical error (±)
1	0-2	e-1	0.8232	1	0.0404	1
	4-6	e-2	0.9353	5	0.0439	1
	8-10	e-3	0.7798	9	0.0367	1
	12-14	e-4	0.6677	13	0.0435	1
	18-20	e-5	0.6184	17	0.037	1
	20-25	e-6	0.3845	22.5	0.024	2.5
	30-35	e-7	0.4597	32.5	0.0267	2.5
	40-45	e-8	0.3055	42.5	0.0217	2.5
	50-55	o-1	0.3981	52.5	0.024	2.5
	60-65	o-2	0.3705	62.5	0.0235	2.5
2	0-2	o-7	0.5209	1	0.059	1
	4-6	e-1	0.4268	5	0.0236	1
	6-8	e-2	0.3806	7	0.0201	1
	8-10	e-3	0.3498	9	0.0204	1
	10-12	e-4	0.3491	11	0.0193	1
	12-14	e-5	0.2381	13	0.0145	1
	16-18	e-6	0.2464	17	0.0161	1
	20-25	e-7	0.2663	22.5	0.0177	2.5
	30-35	e-8	0.2356	42.5	0.0157	2.5
	45-50	o-2	0.1989	47.5	0.0174	2.5
3	0-2	e-1	0.3912	1	0.0218	1
	4-6	e-2	0.4369	5	0.0231	1
	8-10	e-3	0.271	9	0.0177	1
	12-14	e-4	0.4623	13	0.0256	1
	16-18	e-5	0.3004	17	0.0201	1
	20-25	e-6	0.2136	22.5	0.0144	2.5
	30-35	e-7	0.2123	32.5	0.0149	2.5
	40-45	e-8	0.2357	42.5	0.0159	2.5
	50-55	o-1	0.1347	52.5	0.0101	2.5
	60-65	o-2	0.1384	62.5	0.0108	2.5
	65-70	o-3	0.1081	67.5	0.05	2.5
4	0-2	e-1	0.7322	1	0.0368	1
	2-4	e-2	0.856	3	0.041	1
	4-6	e-3	1.0609	5	0.0485	1
	6-8	e-4	1.1038	7	0.048	1
	8-10	e-5	1.1278	9	0.0544	1
	10-12	e-6	1.1104	11	0.0482	1
	12-14	e-7	1.056	13	0.0508	1
	14-16	e-8	1.1031	15	0.0536	1
	16-18	o-1	1.0945	17	0.0498	1
	18-20	o-2	0.6896	19	0.0319	1
	20-25	o-3	0.5101	22.5	0.0346	2.5
	25-30	o-4	0.4491	27.5	0.0245	2.5
	30-35	e-1	0.7008	32.5	0.118	2.5
	40-45	e-2	0.4864	42.5	0.0253	2.5
	45-50	e-3	0.4712	47.5	0.0277	2.5
	50-55	e-4	0.4206	52.5	0.0242	2.5
	55-60	e-5	0.353	57.5	0.0207	2.5
	60-65	e-6	0.3811	62.5	0.0238	2.5
	65-70	e-7	0.3241	67.5	0.0224	2.5
	70-80	e-8	0.2969	75	0.0195	5
	80-90	o-1	0.2585	85	0.0166	5
	90-100	o-2	0.1926	95	0.0149	5

Site	Depth interval (cm)	^{137}Cs counts g^{-1}	Depth plotted (cm)	Horizontal error (±)	Vertical error (±)
1	0-1	0.001945	0.5	0.000161	0.5
	10-11	0.001346	10.5	0.0001332	0.5
	20-21	0.003814	20.5	0.0002177	0.5
	30-31	0.003725	30.5	0.0002275	0.5
	40-41	0.003856	40.5	0.0001767	0.5
	42-43	0.003434	42.5	0.0002155	0.5
	45-46	0.00332	45.5	0.0002194	0.5
	48-49	0.004431	48.5	0.0002517	0.5
	49-50	0.006482	49.5	0.0003073	0.5
	50-51	0.005946	50.5	0.0002995	0.5
	51-52	0.006712	51.5	0.0003109	0.5
	54-55	0.004807	54.5	0.0002431	0.5